Diffusion Coefficients in Hydrocarbon Systems

The Ethane–*n*-Decane System in the Liquid Phase

H. H. REAMER, J. H. LOWER, and B. H. Sage
Chemical Engineering Laboratory, California Institute of Technology, Pasadena, Calif.

Molecular transport in the liquid phase of the ethane–*n*-decane system was investigated at pressures up to 1000 p.s.i.a., in the temperature interval between 40° and 400° F. The results are reported in terms of the Chapman-Cowling diffusion coefficient. This coefficient was chosen because it exhibits smaller variation with change in state of binary hydrocarbon liquids than is encountered with the Fick diffusion coefficient. The method of evaluation of the Chapman-Cowling coefficient from the experimental measurements is presented.

INVESTIGATION of the molecular transport of the lighter hydrocarbons in the liquid phase of hydrocarbon systems was initiated by Lacey and coworkers (*2, 4, 5, 8*). These earlier measurements have been supplemented by experimental studies extending to higher pressures and temperatures and covering a range of binary systems. The transport of ethane in the liquid phase of the ethane–*n*-pentane system has been investigated (*12*). The present study is concerned with the molecular transport in the liquid phase of the ethane–*n*-decane system at pressures up to 1000 p.s.i.a. and in the temperature interval between 40° and 400° F.

EXPERIMENTAL METHODS

Ethane was introduced, at a known rate, into an isochoric chamber containing a heterogeneous mixture of ethane and *n*-decane which initially was at physical equilibrium. The pressure was raised a predetermined amount by addition of ethane, and the quantity of ethane required to maintain the system under isobaric conditions at the higher pressure was determined as a function of time.

The equipment has been described in some detail (*10, 11*). Thin-walled vertical steel tubes were provided in the isochoric chamber to decrease the influence of local accelerations upon the molecular transport. The temperature was known relative to the international platinum scale within 0.02° F. The pressure within the isochoric vessel was measured by a balance involving a piston-cylinder combination and was known within 0.1 p.s.i. or 0.05%, whichever was the larger measure of uncertainty. In order to maintain isobaric conditions with high precision, a manostat was employed (*14*). The ethane was introduced by a mechanical injector (*10*), and the position of the injector was recorded automatically in a digital fashion as a function of time (*11*). The rate of introduction of ethane by the injector was controlled from the output of the manostat, and variations in pressure during a diffusion measurement were not more than 0.05 p.s.i.

Earlier (*10*), an analysis was presented which led to an evaluation of the Fick diffusion coefficient from measurements carried out with the equipment employed here. The analysis included a number of simplifying assumptions concerning the behavior of the system, particularly in regard to the transport of the less volatile component between phases. For this reason, carrying out a more precise analysis of the experimental measurements and reporting the results in terms of the Chapman-Cowling (*3*) diffusion coefficient rather than the Fick coefficient were undertaken.

In the following analysis, the vessel in which the transient diffusion measurements are carried out is isochoric (*10*). The total rate of introduction of component *k* may be related to the rate at which it enters the liquid and gas phases by:

$$\underline{m}_{kc} = \underline{m}_{kl} + \underline{m}_{kg} \tag{1}$$

A similar relationship applies for component *j*,

$$\underline{m}_{jc} = 0 = \underline{m}_{jl} + \underline{m}_{jg} \tag{2}$$

If local equilibrium at the gas-liquid interface is assumed, the rate of addition of each of the components to the gas phase may be established from

$$\begin{aligned} \underline{m}_{kg} &= \sigma_{kd}\underline{V}_g = -\,\sigma_{kd}\underline{V}_l \\ &= -(\sigma_{kd}\overline{V}^*_{kl}\underline{m}_{kl} + \sigma_{kd}\,\overline{V}^*_{jl}\underline{m}_{jl}) \end{aligned} \tag{3}$$

and

$$\begin{aligned} \underline{m}_{jg} &= \sigma_{jd}\underline{V}_g = -\,\sigma_{jd}\underline{V}_l \\ &= -(\sigma_{jd}\overline{V}^*_{kl}\underline{m}_{kl} + \sigma_{jd}\overline{V}^*_{jl}\underline{m}_{jl}) \end{aligned} \tag{4}$$

The third equalities of Equations 3 and 4 assume that the partial volume of the components in the liquid phase is invariant throughout the change in state associated with a single measurement. Throughout the foregoing expressions, the total quantity of material entering the phase has been considered. Similar expressions could have been derived for a unit cross-sectional area.

If Equations 1 and 2 are combined with the second equalities of Equations 3 and 4, then

$$\underline{m}_{kl} - \underline{m}_{kc} = \sigma_{kd}\overline{V}^*_{kl}\underline{m}_{kl} + \sigma_{kd}\overline{V}^*_{jl}\,\frac{\sigma_{jd}\overline{V}^*_{kl}}{1 - \sigma_{jd}\overline{V}^*_{jl}}\,\underline{m}_{kl} \tag{5}$$

Further rearrangement and considering the flux per unit area results in

$$m_{kli} = \frac{\underline{m}_{kl}}{A_i} = \frac{\underline{m}_{kc}}{A_i}\left[1 + \frac{\sigma_{kd}\overline{V}^*_{kl}}{1 - \sigma_{jd}\overline{V}^*_{jl} - \sigma_{kd}\overline{V}^*_{kl}}\right] \tag{6}$$

Equation 6 also uses the fact that the interfacial fluxes are identical with the rate of change of components *k* and *j* in the liquid phase. For component *j* there is obtained

$$m_{jli} = \frac{\underline{m}_{jl}}{A_i} = \frac{\underline{m}_{kc}}{A_i}\left[\frac{\sigma_{jd}\overline{V}^*_{kl}}{1 - \sigma_{jd}\overline{V}^*_{jl} - \sigma_{kd}\overline{V}^*_{kl}}\right] \tag{7}$$

Equations 6 and 7 represent relationships between the flux of components *k* and *j* across the interface with the rate of addition of component *k* to the cell per unit net cross-sectional area of the cell normal to the diffusion process.

The derivation of these equations, as stated earlier, assumes local equilibrium (*6*) at the interface and constant partial volumes in the liquid phase during the change in states encountered in the diffusion process.

The treatment of diffusion processes under conditions of constant total volume of the phase and constant diffusion coefficient produces a simple and well-known solution. The restriction of no change in total volume of the liquid phase as a result of diffusion alone, makes it necessary to determine at the interface the fluxes of components k and j with respect to a frame of reference fixed with respect to the isochoric vessel. The interfacial velocity regarding the fluxes across that plane is established by:

$$u_i = -\, m_{kli}\overline{V}^*_{kl} - m_{jli}\overline{V}^*_{jl} \tag{8}$$

Combining with Equations 6 and 7 results in

$$u_i = -\,\frac{\underline{m}_{kc}}{A_i}\left[\frac{\overline{V}^*_{kl}}{1-\overline{V}^*_{kl}\sigma_{kd}-\overline{V}^*_{jl}\sigma_{jd}}\right] \tag{9}$$

The flux relative to a frame of reference fixed with respect to the cell at the interface is related to the interfacial flux by

$$m_{kl} = m_{kli} + u_i\,\sigma_{kb} \tag{10}$$

A combination of Equations 6, 9, and 10 followed by rearrangement results in

$$\underline{m}_{kl} = \frac{\underline{m}_{kc}}{A_i}\left[1-\frac{\overline{V}^*_{kl}(\sigma_{kb}-\sigma_{kd})}{1-\overline{V}^*_{kl}\sigma_{kd}-\overline{V}^*_{jl}\sigma_{jd}}\right] \tag{11}$$

The corresponding equation to Equation 11 for component j assumes the form

$$m_{jl} = \frac{\underline{m}_{kc}}{A_i}\left[\frac{\sigma_{jd}\overline{V}^*_{kl}-\sigma_{jb}\overline{V}^*_{kl}}{1-\sigma_{jd}\overline{V}^*_{jl}-\sigma_{kd}\overline{V}^*_{kl}}\right] \tag{12}$$

Solving for the ratio of the fluxes as described for component k by Equation 11 and for component j by Equation 12, there results after rearrangement

$$\frac{m_{kl}}{m_{jl}} = -\,\frac{\overline{V}^*_{jl}}{\overline{V}^*_{kl}} \tag{13}$$

When partial volumes are constant, the ratio of the fluxes of the two components throughout the liquid phase of the diffusion cell is a constant. Equations 11 and 12 relate the fluxes of components k and j relative to a fixed frame of reference at the interface to the rate of addition of component k to the isochoric vessel as a whole and involve no new assumptions.

The flux of components k and j relative to a frame of reference fixed with respect to the diffusion cell may be expressed in terms of the Chapman-Cowling diffusion coefficient by the defining relationships:

$$m_{kl} = u\,\sigma_k - \sigma\,D_{Ckj}\,\frac{\partial n_k}{\partial x} \tag{14}$$

$$m_{jl} = u\,\sigma_j - \sigma\,D_{Ckj}\,\frac{\partial n_j}{\partial x} = u\,\sigma_j + \sigma\,D_{Ckj}\,\frac{\partial n_k}{\partial x} \tag{15}$$

Combining Equations 13, 14, and 15 yields

$$m_{kl} = -\,\sigma^2\,\overline{V}^*_j D_{Ckj}\,\frac{\partial n_k}{\partial x} \tag{16}$$

The concentration σ_k is defined by

$$\sigma_k = n_k\sigma \tag{17}$$

Differentiation yields

$$\frac{d\sigma_k}{dn_k} = \sigma + n_k\,\frac{\partial\sigma}{\partial n_k} = \sigma - \sigma^2\,n_k\,\frac{\partial V}{\partial n_k} \tag{18}$$

Rearranging Equation 18 results in

$$\frac{\partial\sigma_k}{\partial n_k} = \sigma^2\left(V - n_k\left(\frac{\partial V}{\partial n_k}\right)_{T,P}\right) = \sigma^2\overline{V}_j \tag{19}$$

The second equality results from a well-known relation (*7*) between systems of unit and variable weight. A combination of Equation 16 and Equation 19 results in

$$m_{kl} = -\,D_{Ckj}\,\frac{\partial\sigma_k}{\partial x} \tag{20}$$

For the conditions set forth, it is apparent from earlier discussions (*10*) that

$$D_{Ckj} = \frac{\pi\,\underline{m}^2_{kl}}{4A_j^2\Theta(\sigma_{kb}-\sigma_{kbo})^2} \tag{21}$$

In Equation 21 the concentration σ_{kbo} is the equilibrium concentration of component k at the initial state, while the quantity σ_{kb} is the equilibrium concentration of this component at the state of the interface during the diffusion measurements. It is again emphasized that, with the assumption of constant values of the partial specific volumes in the liquid phase and an infinite length of liquid phase, there is no change in the total volume as a result of the diffusion process per se, and all changes in the total volume of the liquid phase occur at the interface as a result of the interfacial fluxes. A combination of Equations 11 and 21 results in the following expression for the Chapman-Cowling diffusion coefficient in terms of the experimentally measured quantities (*10*):

$$D_{Ckj} = \left[\frac{\pi\,\underline{m}^2_{kc}}{4A_i^2\Theta\,(\sigma_{kb}-\sigma_{kbo})^2}\right]\left[1-\frac{\overline{V}^*_{kl}\,(\sigma_{kb}-\sigma_{kd})}{1-\overline{V}^*_{kl}\,\sigma_{kd}-\overline{V}^*_{jl}\,\sigma_{jd}}\right]^2 \tag{22}$$

A more elaborate mathematical analysis employing a coordinate system based at the interface yields the same expression for the Chapman-Cowling coefficient that has been employed in the evaluation of the experimental results herein reported. Adequate volumetric data (*9*, *13*) are available to permit the utilization of Equation 23 to evaluate the corresponding Fick coefficients for each of the components whenever this appears feasible.

The second bracketed term of Equation 22 involves only equilibrium data and the values are shown in Figure 1 as a function of state. The information is based on available volumetric and phase equilibrium data (*9*, *13*). The value of the factor employed was established, in each instance, for the state at which the diffusion measurement was made. These methods of analysis and the associated corrections become unwieldy to apply as the critical state of the binary system is approached at the temperature of measurement. The following general relationships between the Fick diffusion coefficients and the Chapman-Cowling coefficient exist:

$$D_{Ckj} = \frac{\overline{V}_j}{V_l}\,D_{Fk} = \frac{\overline{V}_k}{V_l}\,D_{Fj} \tag{23}$$

MATERIALS

The ethane was of research grade (Phillips Petroleum Co.) contained less than 0.001 mole fraction of impurities. This degree of purity was confirmed by mass spectrographic analysis.

The *n*-decane (Phillips Petroleum Co.) was reported to contain less than 0.01 mole fraction of impurities. The refractive index relative to the D-lines of sodium at 77° F. was 1.4097 as compared with a value of 1.40967 reported (*1*) for an air-saturated sample at the same temperature. The specific weight of the sample of *n*-decane at atmospheric pressure at 77° F. was 45.3546 pounds per cubic foot which compares satisfactorily with a value of 45.337 reported (*1*) for an air-saturated sample at the same temperature. The above comparisons indicate that the *n*-decane probably contained less impurities than the value indicated by the vendor. The ethane and *n*-decane were introduced into the equipment by conventional high-vacuum techniques.

EXPERIMENTAL RESULTS

Typical experimental results for one set of measurements are shown in Table I. These measurements were carried out at a temperature of 160° F. and the initial equilibrium pressure was 258.4 p.s.i.a. The molecular transport measurements were carried out at a pressure of 294.7 p.s.i.a. The weight of ethane added to the isochoric vessel is recorded for a series of times in Table I. These data are plotted in Figure 2. The standard error of estimate, σ, of the experimental points from a straight line relating the weight of ethane added to the square root of time was 0.84×10^{-6} pound. Such straight lines were fitted to the experimental data by conventional least squares techniques. As expected (*8*), deviation from the straight line becomes significant after more than one-half the weight of ethane required to reach equilibrium has been introduced into the isochoric cell. When the cell was agitated a rapid increase in the weight of ethane occurred in order to reach equilibrium.

The experimental results are summarized in Table II. A total of 30 measurements similar to those shown in Figure 2 were obtained in the course of this investigation. The initial equilibrium pressure and the higher isobaric value maintained during the transport measurements are recorded in Table II, along with the composition and concentration of ethane at the interface. The standard error of estimate of the experimental measurements from the straight line illustrated in Figure 2 is indicated for each set of measurements. Likewise, the correction factor for each set of conditions has been included, along with values of the Chapman-Cowling diffusion coefficient for the ethane-*n*-decane system in the liquid phase. As indicated, values of the Fick diffusion coefficient for ethane and *n*-decane may be calculated from these volumetric data by application of Equation 23.

The influence of pressure on the Chapman-Cowling diffusion coefficient in the liquid phase of the ethane-*n*-decane system is shown in Figure 3. Conventional least squares techniques were employed in fitting these curves to the experimental points. The standard error of estimate of the experimental points from the smooth curves was 0.62×10^{-8}

Table I. Typical Experimental Measurements at 160° F.

Pressure, p.s.i.a.,	258.4[a]	294.7[b]
Weight fraction ethane,	0.074[a]	0.086[b]

Time, Sec.	Weight of Ethane Added,[c] Lb.
200	0
400	0.302×10^{-6}
600	15.268
800	27.506
1000	36.573
1200	45.641
2000	77.076
2400	89.469
2800	102.466
3206	113.649
3600	122.112
4000	133.296
4400	143.573
4800	150.412
5200	162.011
5600	167.451
6000	176.217
6400	184.680
6800	189.516
7200	197.677
7600	203.540
8000	208.256
8100	342.761
8200	367.849
8300	368.453
8600	368.453
9200	369.965
9500	369.965
9800	369.965

[a] Initial equilibrium pressure and composition. [b] Constant operating pressure and associated composition at interface during transport. [c] Weight added to heterogeneous isochoric system.

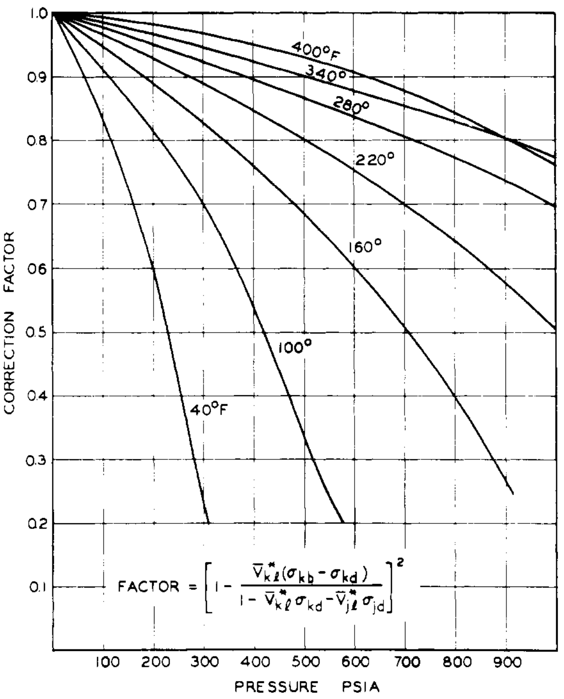

Figure 1. Correction factor for the ethane–*n*-decane system

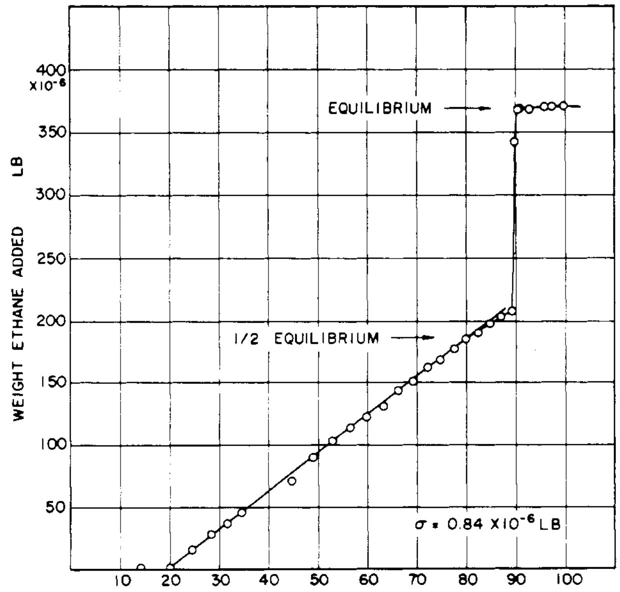

Figure 2. Typical experimental measurements at 160° F.

Table II. Summary of Experimental Results

Pressure, P.S.I.A.		Comp., Ethane Wt. Fraction	Concn., Ethane Lb./Cu.Ft.	$(\Delta \underline{m}_{kc})^2/\theta$ Lb.^{2} Sec.[a]	Standard Error of Estimate, Lb.	Correction Factor	Chapman-Cowling Diffusion Coefficient Sq.Ft./Sec.
Initial	Final						
				40° F.			
149.6	164.3	0.135	5.820	14.11×10^{-12}	1.57×10^{-6}	0.692	4.10×10^{-8}
247.7	262.2	0.304	12.050	63.03	2.01	0.368	4.45
				100° F.			
38.9	47.4	0.017	0.780	0.52	0.40	0.960	5.35
61.2	72.6	0.027	1.185	1.03	1.04	0.938	5.67
226.5	251.3	0.114	4.825	11.12	1.49	0.757	5.79
313.6	345.6	0.180	7.165	32.49	2.21	0.629	5.80
409.5	448.6	0.274	10.300	86.68	3.93	0.443	5.46
				160° F.			
125.1	150.8	0.040	1.700	4.35	3.68	0.918	7.82
258.4	294.7	0.086	3.530	9.27	0.84	0.830	6.52
350.9	398.2	0.125	4.960	21.95	1.49	0.759	7.85
453.1	522.0	0.179	6.780	56.87	1.97	0.666	7.62
550.8	629.2	0.234	8.540	94.03	4.51	0.573	6.52
696.8	770.0	0.323	11.080	122.41	14.73	0.430	6.21
				220° F.			
88.7	111.1	0.021	0.875	1.58	1.03	0.963	9.22
204.7	254.5	0.053	2.083	9.67	0.64	0.908	9.99
452.1	549.5	0.130	4.875	52.94	1.16	0.778	9.76
602.2	706.1	0.180	6.480	73.70	2.95	0.695	9.47
994.5	1070.0	0.326	10.450	65.58	7.01	0.443	9.15
				280° F.			
204.2	254.6	0.042	1.610	7.66	0.66	0.936	13.09
310.4	383.5	0.066	2.483	18.24	0.33	0.900	13.47
399.2	489.3	0.086	3.202	25.47	0.71	0.869	12.43
498.0	590.2	0.108	3.911	32.08	0.78	0.839	13.66
597.8	687.0	0.130	4.589	30.04	1.42	0.810	13.14
				340° F.			
126.4	159.4	0.019	0.737	2.03	0.81	0.974	15.01
241.9	302.1	0.041	1.490	8.60	0.47	0.946	16.55
355.4	439.7	0.063	2.248	17.33	0.44	0.916	15.34
453.4	555.9	0.084	2.913	28.89	1.40	0.888	15.43
				400° F.			
418.8	516.9	0.064	2.120	19.83	1.20	0.927	19.22
528.4	629.2	0.082	2.650	22.62	0.96	0.899	18.96
648.6	746.4	0.101	3.222	20.88	1.57	0.863	17.03

[a] Effective cross-sectional area = 0.019187 sq. ft.

Table III. Chapman-Cowling Diffusion Coefficients

Pressure, P.S.I.A.	Comp., Ethane Wt. Fraction	Specific Volume, Cu.Ft./Lb.	Concn., Ethane Lb./Cu.Ft.	Partial Volume Cu.Ft./Lb.		Chapman-Cowling Diffusion Coefficient Sq.Ft./Sec.
				Ethane	*n*-Decane	
			40° F.			
0.004[a]	0	0.0215	0	...	0.0215	4.47×10^{-8}
100	0.068	0.0225	3.037	0.0352	0.0215	4 46
200	0.184	0.0240	7.688	0.0346	0.0216	4.45
300	0.424	0.0274	15.47	0.0367	0.0205	4.44[b]
385[c]	1.000	0.0399	25.06	0.0399	...	4.4
			100° F.			
0.073[a]	0	0.0222	0	...	0.0222	5.75
100	0.038	0.0229	1.644	0.0382	0.0222	5.71
200	0.085	0.0236	3.608	0.0379	0.0222	5.68
300	0.146	0.0245	5.957	0.0378	0.0222	5.64
400	0.226	0.0258	8.766	0.0378	0.0221	5.61
500	0.334	0.0276	12.08	0.0392	0.0214	5.55[b]
600	0.485	0.0306	15.84	0.0428	0.0194	5.51
700	0.706	0.0370	19.10	0.0497	...	5.5
778[d]	0.977	0.0699	13.97	...	...	5.4
			160° F.			
0.4[a]	0	0.0232	0	...	0.0232	7.76
100	0.026	0.0236	1.093	0.0410	0.0231	7.63
200	0.055	0.0241	2.284	0.0411	0.0231	7.54
300	0.088	0.0247	3.584	0.0414	0.0230	7.44
400	0.126	0.0253	4.976	0.0417	0.0230	7.34
500	0.169	0.0261	6.455	0.0420	0.0229	7.25
600	0.218	0.0270	8.069	0.0425	0.0227	7.16

(Continued on page 58)

Table III. Chapman-Cowling Diffusion Coefficients *(Continued)*

Press., P.S.I.A.	Comp., Ethane Wt. Fraction	Specific Volume, Cu.Ft./Lb.	Concn., Ethane Lb./Cu.Ft.	Partial Volume Cu. Ft./Lb.		Chapman-Cowling Diffusion Coefficient (Sq. Ft./Sec.)
				Ethane	*n*-Decane	
			160° F.			
700	0.276	0.0281	9.803	0.0433	0.0222	7.02×10^{-8}
800	0.344	0.0296	11.63	0.0450	0.0212	6.90[b]
900	0.425	0.0315	13.48	0.0479	0.0188	6.76
1000	0.519	0.0344	15.11	0.0541	0.0144	6.60
			220° F.			
1.59[a]	0	0.0242	0	...	0.0242	10.27
100	0.019	0.0245	0.772	0.0451	0.0241	10.16
200	0.040	0.0249	1.610	0.0454	0.0240	10.03
300	0.063	0.0253	2.496	0.0457	0.0239	9.91
400	0.088	0.0258	3.423	0.0462	0.0238	9.78
500	0.116	0.0264	4.379	0.0467	0.0237	9.67
600	0.146	0.0271	5.384	0.0473	0.0236	9.54
700	0.178	0.0277	6.416	0.0481	0.0234	9.43
800	0.213	0.0285	7.467	0.0491	0.0232	9.29
900	0.251	0.0293	8.562	0.0504	0.0227	9.12
1000	0.293	0.0303	9.681	0.0520	0.0218	8.91
			280° F.			
5.08[a]	0	0.0252	0	...	0.0252	13.25
100	0.015	0.0255	0.592	0.0508	0.0251	13.07
200	0.032	0.0259	1.239	0.0511	0.0250	12.91
300	0.050	0.0263	1.909	0.0514	0.0249	12.72
400	0.069	0.0267	2.592	0.0518	0.0248	12.56
500	0.089	0.0272	3.274	0.0522	0.0247	12.39
600	0.110	0.0277	3.972	0.0527	0.0246	12.21
700	0.132	0.0283	4.678	0.0534	0.0245	12.05[b]
800	0.156	0.0289	5.420	0.0542	0.0242	11.88
900	0.182	0.0296	6.151	0.0552	0.0239	11.69
1000	0.210	0.0303	6.922	0.0566	0.0233	11.50
			340° F.			
13.49[a]	0	0.0263	0	...	0.0263	16.36
100	0.012	0.0267	0.431	0.0591	0.0262	16.15
200	0.026	0.0270	0.947	0.0595	0.0262	15.91
300	0.041	0.0275	1.480	0.0600	0.0260	15.69
400	0.057	0.0280	2.030	0.0604	0.0260	15.47
500	0.074	0.0285	2.592	0.0609	0.0258	15.26
600	0.092	0.0290	3.161	0.0615	0.0257	15.02[b]
700	0.110	0.0295	3.735	0.0620	0.0255	14.81
800	0.130	0.0301	4.306	0.0627	0.0252	14.60
900	0.150	0.0307	4.871	0.0640	0.0246	14.39
1000	0.171	0.0314	5.444	0.0659	0.0238	14.13
			400° F.			
31.19[a]	0	0.0278	0	...	0.0278	19.55
100	0.008	0.0281	0.277	0.0672	0.0278	19.35
200	0.020	0.0285	0.694	0.0695	0.0276	19.13
300	0.033	0.0290	1.131	0.0718	0.0274	18.86
400	0.047	0.0295	1.582	0.0743	0.0272	18.55
500	0.061	0.0300	2.042	0.0771	0.0269	18.27
600	0.076	0.0305	2.506	0.0801	0.0265	18.00
700	0.093	0.0312	2.994	0.0840	0.0260	17.72
800	0.111	0.0319	3.480	0.0892	0.0252	17.48[b]
900	0.130	0.0328	3.962	0.0954	0.0243	17.19
1000	0.149	0.0337	4.413	0.1021	0.0232	16.91

[a] Vapor pressure *n*-decane. [b] Values at this and higher pressures were extrapolated from data at lower pressures.

[c] Vapor pressure ethane.

[d] Critical pressure of ethane–*n*-decane system.

square foot per second. The average deviation of the experimental points with regard to sign was 0.08×10^{-8} square foot per second. The dashed portions of the curves involve markedly greater uncertainty than the region shown by the full curves, which corresponds to the domain of experimental measurements. The effect of temperature upon the Chapman-Cowling diffusion coefficient is shown in Figure 4. Smooth values of the Chapman-Cowling diffusion coefficient with corresponding values of the composition and concentration of ethane in the liquid phase are reported in Table III. In addition, values of the specific volume of the bubble-point liquid and the partial volumes of both components are included.

ACKNOWLEDGMENT

The analysis of the experimental work was carried out with the assistance of G.N. Richter, Virginia Berry contributed materially to the calculations, while B. Lawson Miller assisted in the preparation of the manuscript.

NOMENCLATURE

A_i = interfacial area, sq. ft.
D_{Ck_j} = Chapman-Cowling diffusion coefficient for components k and j, sq.ft./sec.
D_F = Fick diffusion coefficient, sq.ft./sec.
d = differential operator

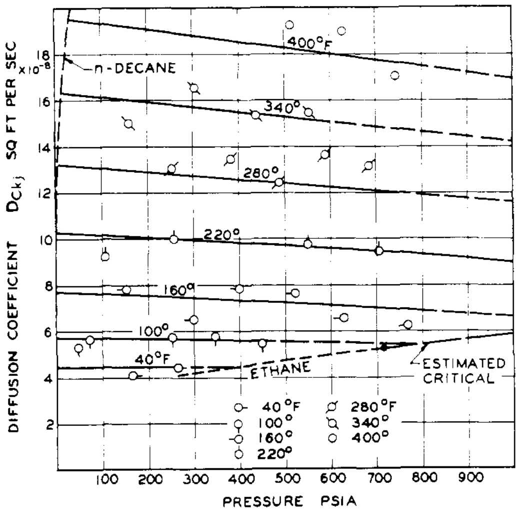

Figure 3. Chapman-Cowling diffusion coefficient

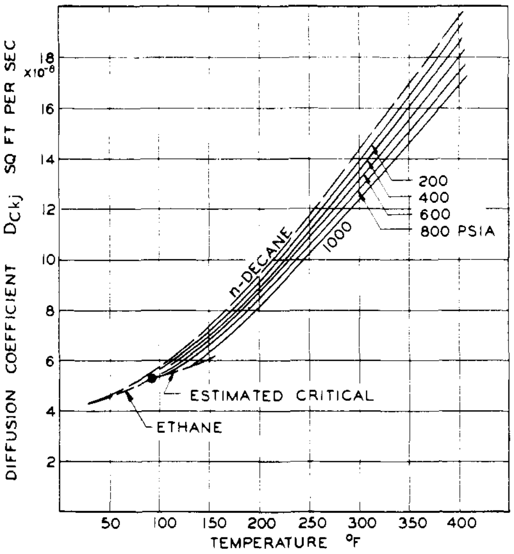

Figure 4. Effect of temperature upon diffusion coefficient

$\underline{m}$ = total material, lb.
$\bar{m}$ = material flux, lb./sec./sq.ft.
$\underline{\underline{m}}$ = total material transport rate, lb./sec.
n = weight fraction
u = local velocity, ft./sec.
u_i = velocity of interface relative to a fixed frame of reference, ft./sec.
V = specific volume, cu.ft./lb.
$\bar{V}$ = partial specific volume of a component, cu.ft./lb.
$\underline{V}$ = rate of change of total volume, cu.ft./sec.
x = length of path, ft.
Δ = difference in
σ = specific weight, lb./cu.ft.
σ_k = concentration of component k, lb./cu.ft.
σ = standard error of estimate
θ = time, sec.
∂ = partial derivative

Subscripts

b = property evaluated at bubble-point conditions
c = transport into the cell
d = property evaluated at dew-point conditions
g = gas phase
i = interface or transport across interface
j = component j, the less volatile, or stagnant, component
k = component k, the more volatile, or diffusing, component
l = liquid phase
o = initial conditions

Superscript

$*$ = average value of a property over the process considered

LITERATURE CITED

(1) Am. Petroleum Inst., Research Project 44, Petroleum Research Laboratory, Carnegie Institute of Technology. "Selected Values of Properties of Hydrocarbons and Related Compounds."
(2) Bertram, E. A., Lacey, W. N., *Ind. Eng. Chem.* **28**, 316 (1936).
(3) Chapman, Sydney, Cowling, T. G., "The Mathematical Theory of Non-Uniform Gases," Cambridge University Press, Cambridge, England, 1939.
(4) Hill, E. S., Lacey, W. N., *Ind. Eng. Chem.* **26**, 1324 (1934).
(5) *Ibid.*, p. 1327.
(6) Kirkwood, J. G., Crawford, B., Jr., *J. Phys. Chem.* **56**, 1048 (1952).
(7) Lewis, G. N., Randall, M., "Thermodynamics and the Free Energy of Chemical Substances," McGraw-Hill, New York, 1923.
(8) Pomeroy, R. D., Lacey, W. N., Scudder, N. F., Stapp, F. P., *Ind. Eng. Chem.* **25**, 1014 (1933).
(9) Reamer, H. H., Berry, V., Sage, B. H., J. CHEM. ENG. DATA, **7**, 486 (1962).
(10) Reamer, H. H., Opfell, J. B., Sage, B. H., *Ind. Eng. Chem.* **48**, 275 (1956).
(11) Reamer, H. H., Sage, B. H., J. CHEM ENG. DATA, **4**, 296 (1959).
(12) *Ibid.*, **6**, 481 (1961).
(13) *Ibid.*, **7**, 161 (1962).
(14) Reamer, H.H., Sage, B.H., *Rev. Sci. Instr.* **29**, 709 (1958).

RECEIVED for review May 20, 1963. Accepted August 8, 1963.